

Crack Paths and Fatigue Strength Assessment of Notched and Un-notched Nodular Cast Iron Components

J. Lepistö, G. Marquis and S. Heinilä

Lappeenranta University of Technology, Department of Mechanical Engineering
P.O. Box 20, FI-53851 LAPPEENRANTA, FINLAND; E-mail: janne.lepisto@lut.fi

***ABSTRACT.** Long-life fatigue tests have been performed on tubular nodular cast iron test specimens using uniaxial tension, torsion and equi-biaxial loading. Observed crack paths were relatively straight for both the tension and torsion load cases but tortuous crack paths were observed for equi-biaxial loading. Fatigue strength data are compared to a Goodman-type fatigue limit criterion. The criterion includes a multiaxial stress state correction that is physically related to the growth of small cracks from notches and small defects. Experimental results obtained from fatigue tests on large thick-walled nodular cast iron structures tested in bending, torsion and combined torsion-bending loading are also presented. Observed crack paths were controlled by both the loading type and the circumferential notch. A mean S–N curve for the component was determined utilising the previously mentioned criterion in order to normalize the test results which included different mean stress levels, principal stress ratios and material strengths.*

INTRODUCTION

Casting offers excellent possibilities with respect to optimization for material usage and functionality. Cast structural components often have complex geometry and are subjected to multiaxial applied loading. Even relatively simple loading cases, like pure torsion, produce a multiaxial stress state. Large components can also contain notches which cause both stress concentrations and multiaxial stresses. These notches, in combination with the external loading, strongly control the fatigue crack paths.

Several successful long-life stress based models for multiaxial fatigue have the same general form and include both a shear stress and a normal stress terms to account for observed mean stress and combined loading effects [1]:

$$\Delta\tau + k\sigma = f \quad (1)$$

Socie [2] and Socie and Marquis [1] have emphasised the need for alternate fatigue damage models depending on whether a material fails predominately due to shear crack growth or due to tensile crack growth. Shear stress based criteria characterised by Eq. (1) have been developed based on observations that, for ductile materials, cyclic shear stresses cause crack nucleation and normal stresses greatly influence fatigue life.

Fatigue of cast iron, on the contrary, has been shown to be largely controlled by normal stresses and thus requires different parameters to correlate fatigue data for different states of stress [2–5].

Even when the applied loading is predominantly torsion, fatigue crack in nodular cast iron form along planes of maximum principal stress amplitude rather than along shear planes. Small cracks nucleate and propagate from naturally occurring inclusions and shrinkage pores [5]. A Goodman-type fatigue limit relation for nodular cast iron has been developed to correlate biaxial and uniaxial data as well as account for mean stress effects [3, 4, 6–8]. The relation can be written

$$\sigma_a = \left(\frac{1}{k_\lambda} - \frac{2 \cdot \sigma_m}{R_m + R_{p0.2}} \right) \cdot \sigma_{a0}, \text{ where} \quad (2)$$

σ_a is the fatigue limit stress amplitude

σ_m is the mean stress on the plane of maximum alternating normal stress

σ_{a0} is the fatigue limit stress amplitude with zero mean stress ($R = -1$)

k_λ is the correction factor due to the biaxial stress state, a function of principal stress ratio $\lambda = \sigma_2 / \sigma_1$. Here $k_\lambda = 1 - 0.25\lambda$

The overall crack path in nodular cast iron can be easily predicted, since the mode I dominates even the nucleation stage. Cracks can thus be assessed as growing along planes of maximum principal stress amplitude. However, some tortuosity can be expected, because graphite nodules and shrinkage pores can change the crack path locally by hindering or accelerating the crack growth and forcing the crack to grow in planes varying slightly from the maximum principal stress amplitude plane.

Notches can also control the crack path in certain loading conditions. Often notches act as a barrier because they cause highly stressed regions in the structure. Cracks often tend to turn back to this highly stressed region. In addition, small cracks can nearly simultaneously nucleate at the notch root. These can coalesce and, when the joined crack is large enough, it can break the barrier made by the notch.

When the loading is equi-biaxial, the crack path is less obvious. In this special case several possible planes exist along which cracks can grow with equal probability. Therefore, a high degree of tortuosity can be expected.

EXPERIMENTS

Materials

Material used in the small test specimen investigations was a nodular cast iron GRP 500 / ISO 1083 cast as 100x100x300 mm ingots. Castings were slow cooled but no post cast heat treatment was performed. Measured tensile properties were $R_{p0.2} = 340$ MPa and $R_m = 620$ MPa. Material used in large cast component experiments was somewhat stronger than that of small specimen tests. Material properties were determined for each tested component separately. These are reported elsewhere [8].

Specimens

Both tubular and solid axial test specimens were used for small test specimen study. Axial polishing using successively finer grades of emery paper and diamond paste was used. More detailed description about the specimens can be found elsewhere [6, 7].

The surfaces of the large cast component test specimens were not specially treated. Highly stressed surfaces were machined. The region of interest contained a circumferential notch, which caused a large stress concentration, especially in bending loading. Test procedures for these components are reported elsewhere [8].

Testing

Stress controlled loading was used for the small tubular specimens. Loading was either cyclic torsion or cyclic biaxial tension, i.e., proportional axial load with internal pressure. The stress ratio for both torsion ($\lambda = -1$) and biaxial ($\lambda = 0.98$) testing was $R = 0.1$. Solid specimens were used for the uniaxial ($\lambda = 0$) tests with a constant tensile mean stress of 182 MPa. Loading continued until a fatigue crack propagated through the 2.0 mm thick wall of the tubular specimens or complete separation of the uniaxial specimens. Tests were interrupted at $2 \cdot 10^6$ fatigue cycles if fatigue failure was not observed. Surface length of the cracks at failure was 3–10 mm.

The large cast components were subjected to several different load cases including bending-only, torsion-only and combinations of torsion and bending. Two of the ten components were tested with constant amplitude non-proportional loading. Two components were subject to proportional variable amplitude loading with a simple over-underload spectrum. In these cases one over- underload cycle was applied for every 10 000 small amplitude ($R = 0$) cycles. The remaining six tests were proportional constant amplitude tests. Most tests were carried out using a stress ratio of $R = 0$. Each specimen included a strain gauge rosette near the expected site of crack initiation. The occurrence of small cracks could be observed relatively early in the fatigue life based on the output of the strain gauge. This point was taken as a criterion for the failure. Tests were interrupted after $1 \cdot 10^6$ cycles if failure was not observed (see [8] for details).

RESULTS AND DISCUSSION

Crack Path Observations

For all stress states tested, fatigue cracks in nodular cast iron specimens nucleated and propagated on maximum principal stress amplitude planes. Typical fatigue cracks under uniaxial tension, torsion and biaxial tension detected in small specimen tests are shown in Fig. 1. Cracks for torsion or tensile loading showed some tortuosity as the crack linked up numerous microstructural features. It is observed, however, that the crack path was well defined. In biaxial loading the cracks grew generally in the plane normal to the hoop stress. In comparison to the torsion or tensile cracks, however, there is significantly more branching. In these tests the stress state was nearly equi-biaxial with the hoop stress only slightly higher than the axial stress, thus the crack nucleation and driving force was nearly equal in all directions.

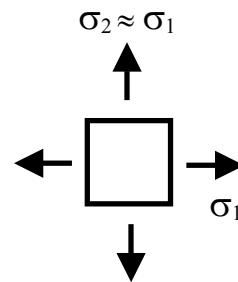
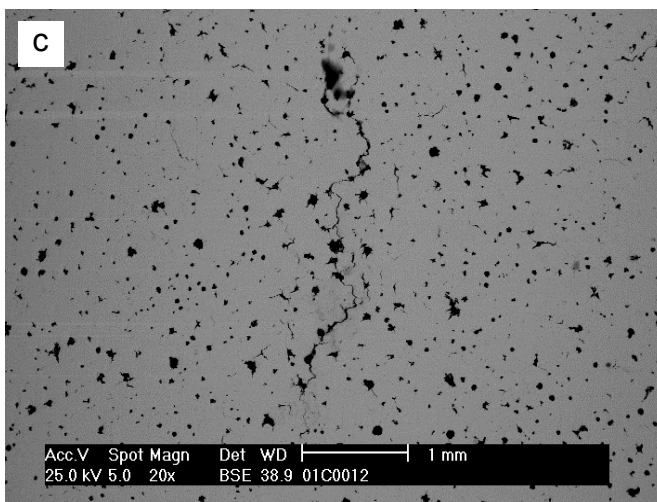
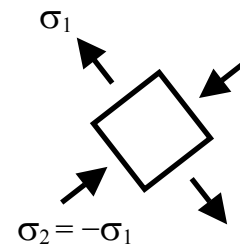
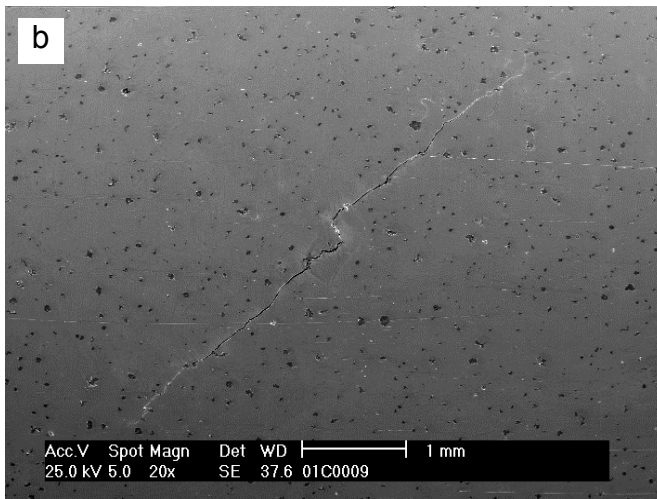
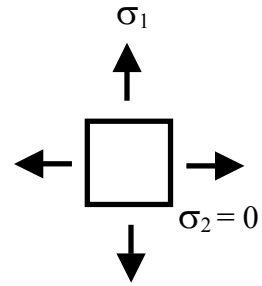
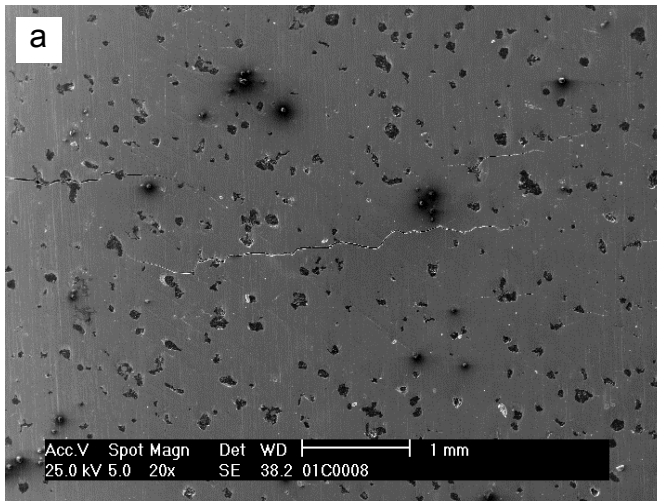


Figure 1. Fatigue cracks observed in small specimen tests during axial tension (a), torsion (b), and biaxial tension loading (c).

Typical fatigue cracks under bending, torsion and torsion-bending found out in large cast component tests are shown in Fig. 2. In the bending case (Fig. 2a), the crack grew along the bottom of the notch. This path was normal to the maximum principal stress amplitude. Figures 2c–d show the crack paths observed for fully reversed torsion. The notch clearly controls the crack path, thus inducing a zigzag crack along the notch bottom. This kind of behaviour is not observed in a torsion test with $R \geq 0$, however. When the loading was torsion-bending with $R = 0$, usually several cracks occurred at the bottom of the notch, see Fig. 2b. The direction of these cracks was very close to the normal of the maximum principal stress amplitude. Since the bending part of the loading in these tests was rather small, it can be expected, that several small cracks initiates at bottom of the notch even when the loading is pure torsion with positive or zero R-value.

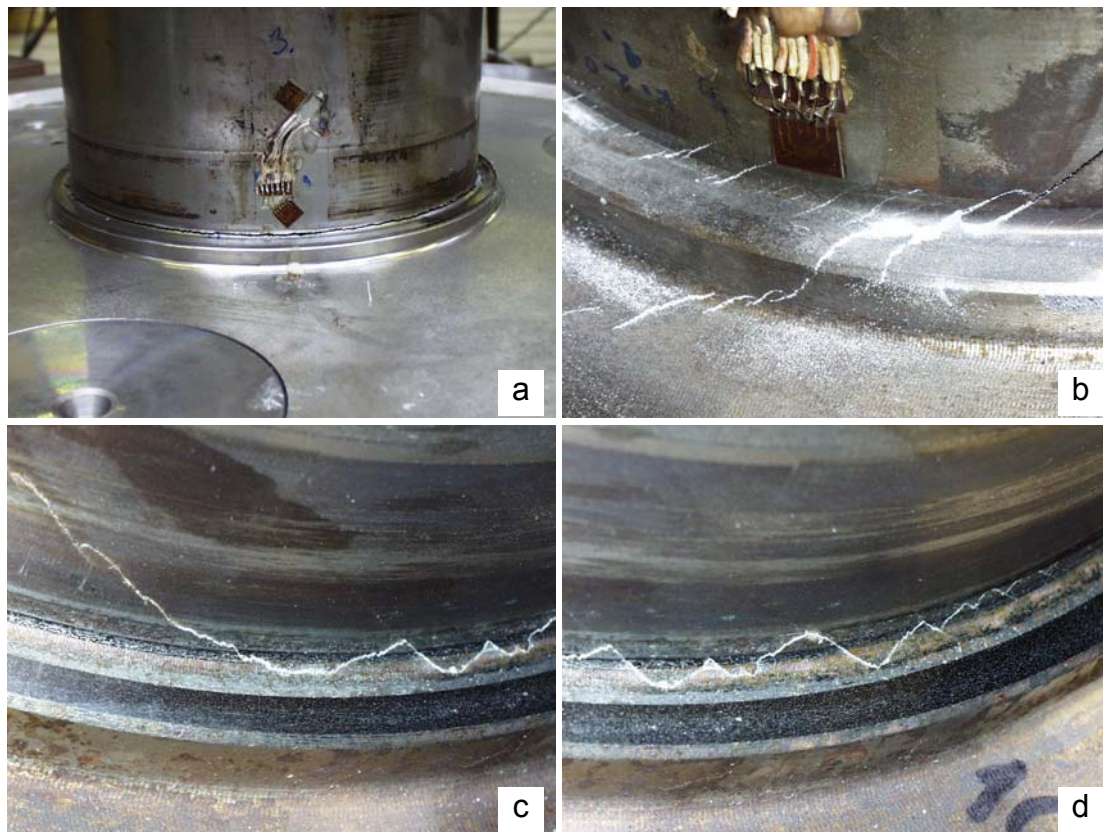


Figure 2. Crack paths observed in large component tests during bending (a), torsion-bending (b), and fully reversed torsion loading (c–d).

Fatigue Life

Details of the fatigue tests for the small specimen investigations have been presented elsewhere [6, 7]. At comparable fatigue lives, the specimens subject to torsion loading failed at noticeably lower stress levels than did the uniaxial tension specimens. The fatigue limit was approximately 78% of the tensile fatigue limit. Under biaxial loading the nodular cast iron had nearly the same fatigue limit as under uniaxial loading.

A mean S–N curve determined for the large cast component is presented in Fig. 3. In this curve, Eq. (2) was utilised in order to normalize the test results, which included different mean stress levels, principal stress ratios and material strengths. Without normalization the scatter would have been much larger. The effect of an occasional over- underload cycle had a dramatic harmful effect on the fatigue strength in these tests. This is the case even though the extra damage produced by the over- underload cycles, when computed using a simple linear damage rule, is negligible. The larger over- underload cycle has no significant influence on the computed equivalent stress amplitude.

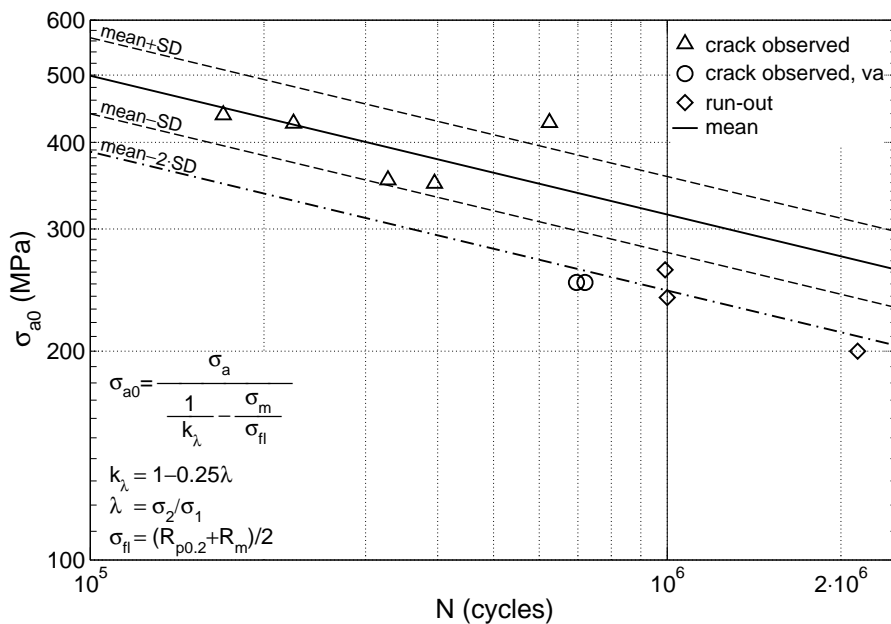


Figure 3. A mean S–N curve for the large cast component.

Effect of Second Principal Stress on Fatigue

While the dominant failure mechanism of the nodular cast iron is due to mode I crack growth, the fatigue limit stresses for torsion and biaxial tension cannot be compared directly to the uniaxial fatigue limit without additional considerations of the stress state. Because failure in nodular iron is controlled by the nucleation and growth of small cracks from inclusions and pores, the second principal stress influences the fatigue strength. Crack driving force near a notch is greater in the case of $\lambda = -1$ (torsion) as compared to uniaxial tension $\lambda = 0$. Consider, for example, the stress concentration factor for a centre hole, which is 3 in uniaxial loading, 4 in torsion, and only 2 for equibiaxial tension. This suggests that the torsion fatigue limit would be only 75% of the uniaxial tensile fatigue limit while the fatigue strength under biaxial tension would be greater than for uniaxial tension. Endo and Murakami [9] and Beretta and Murakami [10] used fracture mechanics arguments to estimate the fatigue strength in torsion to be approximately 80–83% the fatigue limit in tension for materials dominated by mode I failure from small defects. Earlier published work on nodular cast irons has shown that the fatigue limit in torsion is very close to 80% of that in tension [3–6].

The current study with small specimens shows that the fatigue limit for this material is nearly the same for both uniaxial and biaxial tension. Under biaxial loading the crack driving force was nearly equal in all directions so failure in nodular cast iron is not due to nucleation and crack propagation in a single plane but cracks are able to progress freely with no strong directional preference. It is hypothesised that cracks can more easily grow in the direction of microstructural features that with lower fatigue strength. For this reason the fatigue limit in biaxial tension for nodular cast iron is lower than what is expected based on simple elasticity considerations. Increased crack tortuosity is clearly seen in a comparison of cracks in Fig. 1.

Based on the current experiments, Eq. (2) should be modified for nodular cast iron so that k_λ takes on a minimum value of one regardless of the stress state. Figure 4 shows the current data together with previously collected fatigue limit data for nodular cast iron [6]. The line representing Eq. (2) allows the fatigue strength for nodular cast iron components to be estimated based on static tensile properties and the measured endurance limit for one stress state, e.g., fully reversed axial fatigue.

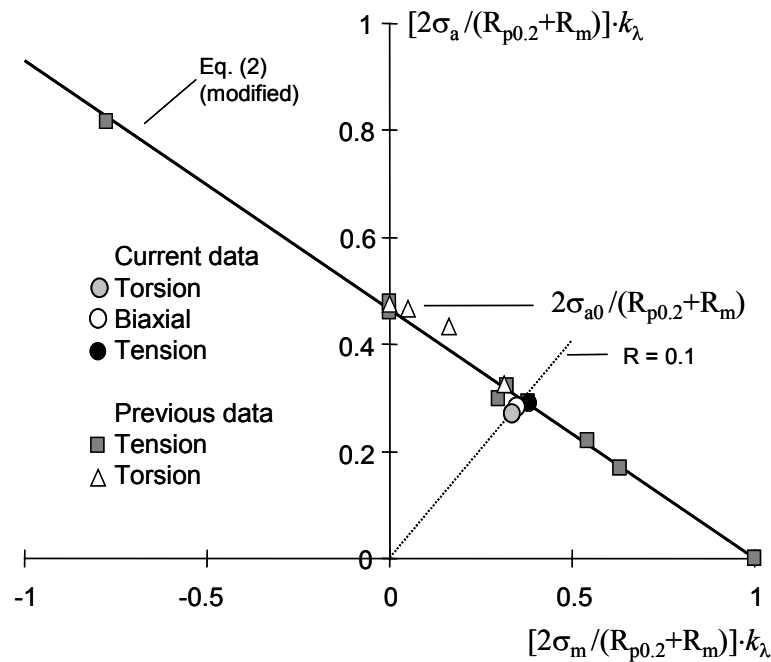


Figure 4. Predicted and measured mean fatigue limit values for nodular cast iron for different mean stresses and stress states.

CONCLUSIONS

Long-life fatigue tests of nodular cast iron have been performed under uniaxial tension, torsion and near equi-biaxial tension. Test data for torsion loading was significantly below the uniaxial fatigue data and the fatigue limit was approximately 78% of the uniaxial fatigue limit. The nodular cast iron had nearly the same fatigue limit as under both biaxial and uniaxial loading.

Fatigue cracks in biaxial fatigue were significantly more tortuous than in either torsion or uniaxial fatigue due to the near equal driving force in all directions. A fatigue limit relation previously developed for this material under tension and torsion loading with a variety of mean stress levels is slightly modified to include biaxial loading.

Usually several small cracks nucleated at the bottom of the notch along the largest principal stress amplitude plane (when $R = 0$). With fully reversed torsion case, also zigzag cracks along the bottom of the notch were observed. These are not expected when $R \geq 0$.

The test results for different loading cases in large component tests could be reduced to a single design line using Eq. (2) to standardise the principal stress amplitude. This takes into account different mean stresses, principal stress ratios and materials in each test.

The test results show clearly, that an occasional over- underload cycle is harmful and reduces the fatigue strength significantly. This is the case even though the extra damage produced by the overload cycles, when computed using a simple linear damage rule, is negligible. The larger over- underload cycle has no significant influence on the computed equivalent stress amplitude.

ACKNOWLEDGEMENTS

This work was partially supported through a grant from the Finnish Academy and the project Fadel/Gjutdesign, which was partially funded by the Nordic Innovation Centre, Wärtsilä Technology, Metso Corp., Componenta Corp. and VTT Industrial Systems. All persons involved are gratefully acknowledged.

REFERENCES

1. Socie, D.F., Marquis, G. B. (2000) *Multiaxial Fatigue*, SAE, Warrendale, PA.
2. Socie, D. F. (1987), *J Eng. Mat. Tech.*, **109**, 293–298.
3. Marquis, G., Socie, D. (2000) *Fract. Engng. Mater. Struct.* **23**, 293.
4. Marquis, G. (2000) In: *ECF 13 Fracture mechanics: applications and challenges*, Fuentes, M., Elices, M., Martin-Meizoso, A, Martinez-Esnaola, J. M. (Eds.), Elsevier Science, Amsterdam.
5. Marquis, G., Rabb, R., Siivonen, L. (1999) In: *Fatigue Crack Growth Thresholds, Endurance Limits, and Design, ASTM STP 1372*, pp. 411–426, Newman, J. C., Piascik, R. (Eds.) ASTM, West Conshohocken.
6. Marquis, G., Solin J. (2001) *Long-Life Fatigue Design of GRP 500 Nodular Cast Iron Components*, VTT research notes 2043, Espoo.
7. Marquis, G. B., Karjalainen-Roikonen, P. (2001) In: *Proceedings of the Sixth International Conference on Biaxial/Multiaxial Fatigue & Fracture*, pp. 151–158, de Freitas, M. M. (Ed.), Lisboa.
8. Lepistö, J. (2005) In: *Competent Design by Castings*, pp. 311–328, Samuelsson, J., Marquis, G., Solin, J. (Eds.), VTT symposium 237, Helsinki.
9. Endo, M., Murakami, Y. (1987) *J Eng. Mat. Tech.* **109**, 124–129.
10. Beretta, S., Murakami, Y. (1998) In: *ECF 12 Fracture from defects*, pp. 55–60 Brown, M. W., de los Rios, E. R., Miller, K. J. (Eds.), EMAS.